Synthesis and structure determination by ultra-fast electron diffraction of the new microporous zeolitic germanosilicate ITQ-62

Lindiane Bieseki, Raquel Simancas, Jose L. Jordá, Pablo J. Bereciartua, Angel Cantín, Jorge Simancas, Sibele B. Pergher, Susana Valencia, Fernando Rey*, Avelino Corma*

Supplementary information

Materials and methods

ICP analyses were performed in a Varian 710-ES device. Solid samples were grinded and then dispersed in 5 ml of 1/1/3 (volumetric ratios) solution of HNO_3 (65% v/v)/HF (40% v/v)/HCl (30% v/v). This dispersion was kept at 40ºC for 12 hours or until a clear solution was formed, and then diluted with MilliQ water up to 60 mL. Calibration curves were built by commercial standard solutions. Nitrogen, carbon and hydrogen (N, C, H) were measured by a Fisons EA1108 elemental analyzer, employing sulfanilamide as standard. TG experiments were performed on a Mettler Toledo TGA/SDTA851e device. Measured samples (ca. 5 mg) were heated up to 800ºC, with a 10ºC/min heating rate under a 20 mL/min of dry air stream. The textural properties of thermally treated and 0.2 - 0.4 mm sieved samples were measured in a Micromeritics ASAP 2020 instrument, with a 400ºC pretreatment under vacuum (10^{-3} Pa) for 12 hours. FESEM images were taken with a ZEISS ULTRA 55 microscope. MAS-NMR measures were performed in a Bruker-400-WB spectrometer at room temperature.

Ammonium containing organic structure directing agent (OSDA)

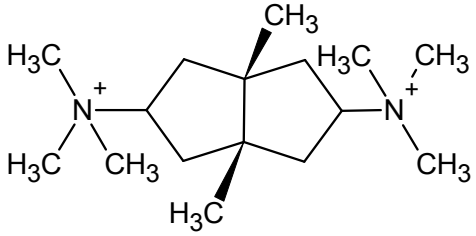

Figure S1: Structure of the N^2,N^2,N^2,N^5,N^5,N^5,3a,6a-octamethyloctahydropentalene-2,5-diammonium cation.

Synthesis of the organic structure directing agent (OSDA), N^2,N^2,N^2,N^5,N^5,N^5,3a,6a-octamethyloctahydropentalene-2,5-diammonium hydroxide

The OSDA was obtained following the method previously described in the literature.[19]

Synthesis of the zeolitic materials

The cation N^2,N^2,N^2,N^5,N^5,N^5,3a,6a-octamethyloctahydropentalene-2,5-diammonium was tested as OSDA in a series of synthesis conditions similar to those used for ITQ-55, but using fluoride media (*Table S1*). The crystallizations yielded to the novel zeolite ITQ-62, as well as ammonium germanate or an amorphous phase as impurities. The zeolite ITQ-62 crystallizes in a narrow range of compositions, and is always obtained with also a small amount of an impurity corresponding to an unknown phase.

Table S1: Synthesis conditions and phases obtained by using N^2,N^2,N^2,N^5,N^5,N^5,3a,6a-octamethyloctahydropentalene-2,5-diammonium hydroxide as OSDA. All syntheses were carried out using the following molar ratios: OSDA/(Si+Ge) = 0.2, NH_4F/(Si+Ge) = 0.4, H_2O/(Si+Ge) = 7 at 423 K for 7 days.

(Si/Ge)	Phases obtained
1	Ammonium germanate + ITQ-62
5	ITQ-62
10	ITQ-62 + amorphous
20	ITQ-62 + amorphous
∞	Amorphous

When replacing NH_4F with HF, the use of a Si/Ge = 5 gel yielded ITQ-62 with small amounts of germanium oxide, while a Si/Ge = 10 produced ITQ-62 with large amounts of an amorphous phase.

Synthesis of the zeolite ITQ-62

In a typical synthesis of zeolite ITQ-62, 0.33 g of GeO_2 and 3.46 g of tetraethylorthosilicate (TEOS) were added to 14.33 g of a 0.268 M aqueous solution of the OSDA. The mixture was stirred at room temperature until total evaporation of the ethanol formed during the hydrolysis of TEOS. Finally, 0.30 g NH_4F in 2 g H_2O was added. The excess of water was evaporated to obtain a synthesis gel with the following molar composition:

$$0.84\ SiO_2 : \textit{0.16}\ GeO_2 : \textit{0.2}\ OSDA(OH)_2 : 0.4\ NH_4F : 7\ H_2O$$

The resulting gel was transferred to Teflon lined stainless-steel autoclaves and heated at 423 K at its autogenous pressure under tumbling (60 rpm) for 7 days. The solid was recovered by filtration and washed exhaustively with distilled hot water. The resulting solid was dried at 373 K overnight to obtain the as-made ITQ-62 zeolite.

Finally, the as-made ITQ-62 zeolite was calcined under a flux of dry air at 923 K, resulting in the decomposition of the occluded OSDA cations and the complete removal of the organic moieties.

Chemical, thermogravimetric and textural analysis of the zeolite ITQ-62

The chemical and elemental analyses of the as-made ITQ-62 are shown in the *table S2*.

The chemical analyses of the ITQ-62 sample gave a Si/Ge ratio of 3.0, lower than the gel composition (Si/Ge=5.2), indicating that part of the Si is not incorporated in the zeolite. The (C/N) ratio of 8.4, compared with the theoretical ratio of 8.0, indicates that (a) the OSDA does not decompose during zeolite crystallization and remains intact inside the channels filling the pores, and (b) NH_4^+cations are not incorporated in the structure. Finally, the (Si+Ge)/N ratio of 22.17 corresponds, after structure determination, to 2 OSDA molecules per unit cell.

The thermogravimetric analyses gave a weight loss of 15.1 % centered at 778 K and the sample continues losing weight until 953 K.

The zeolite ITQ-62 was calcined at 923 K, with a heating rate of 3ºC/min, and under a 60 mL/min air stream for 5 hours. Upon calcination, the BET surface area and the total micropore volume (calculated from the N_2 adsorption isotherm by applying the t-plot method) were 313 m^2/g and 0.19 cm^3/g, respectively (*Figure S2*). The micropore distribution calculated by applying the Horvath-

Kawazoe formalism to the Ar adsorption isotherm of the calcined zeolite ITQ-62 showed a maximum at 6.2 Å (*Figure S2*), which fits well with the size of the monodirectional 12-ring channel. The tridirectional channels with 8-ring openings are not seen because of its small size at the Ar temperature uptake.

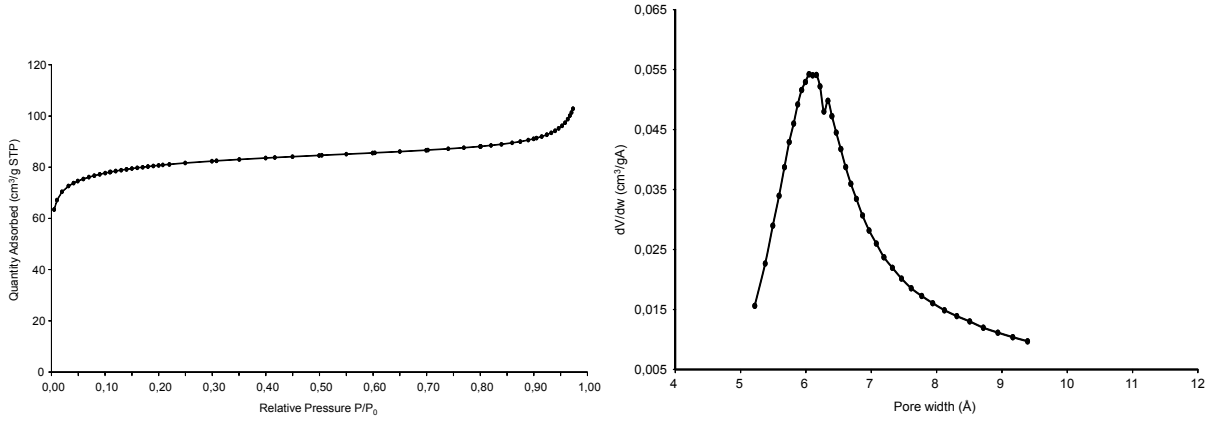

Figure S2: Textural properties of zeolite ITQ-62. Left: Adsorption N_2 isotherm at 77K. Right: Pore diameter distribution determined from the Ar isotherm at 87K.

The ITQ-62 zeolite was obtained as plate-like crystallites with a heterogeneous crystal size distribution, with crystals averaging around 2 x 8 µm and a 0.5-1 µm thickness. Plenty of smaller crystals could are also, probably because of secondary nucleation (*Figure S3*).

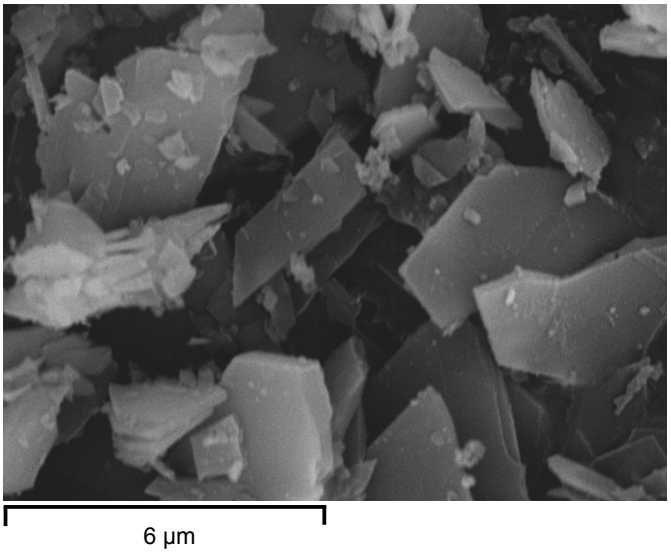

Figure S3: Scanning electron microscope (SEM) microimages of ITQ-62.

Solid state MAS-NMR of the ITQ-62 samples

The cross-polarization (CP) ^{13}C-MAS-NMR spectrum shows five different bands. The comparison of this spectrum with the liquid CP ^{13}C-NMR of the free OSDA shows that the bands obtained in the solid spectrum is the sum of several single signals in the liquid NMR. Also, a small chemical shift displacement is observed in all signals, which could be due to the possible constraint of the molecule in the host zeolite structure. In the end, it can be seen that the OSDA remains intact after the hydrothermal synthesis, as it is also suggested by the chemical analyses.

The ^{19}F-MAS-NMR spectra show several signals corresponding to different chemical environments. The couple of low intensity signals at lower field, around -77.0 and -123.7 ppm could be attributed to the STF and $(NH_4)_2GeF_6$ impurities, respectively.[45] Indeed, the intensity of these two signals varied between different samples, although they were present in all samples measured. Conversely, the signals at higher field fit with fluorine atoms inside D4R cages with different Si and Ge compositions. Thus, the signal at -21.7 ppm could be assigned as Si_7Ge_1 D4R cages, while the signal at -10.9 ppm with its shoulder at -13.7 ppm could be attributed to Si_5Ge_3 D4R cages, or alternatively, a small amount of Si_4Ge_4 D4R cages.[46-48] The deconvolution of this signal gives parameters that suggest the latter option, as the -13.7 ppm signal is wider than the -10.9 ppm signal (~2200 Hz and ~1500 Hz, respectively). This widening could be a sign of a higher number of Ge atoms in the neighborhood of the fluorine atom because of the nuclear spin interaction of the fluorine nuclei with the large quadrupolar moment of the Ge nuclei. Also, when taking in account the Si/Ge ratio of the sample, the relative occupancies of the T atoms in each sample and the relative intensities of each signal in the ^{19}F spectra, the results are more closely related to the bulk composition if this -13.7 ppm signal is considered as Si_4Ge_4 instead of Si_5Ge_3. (Figure S4)

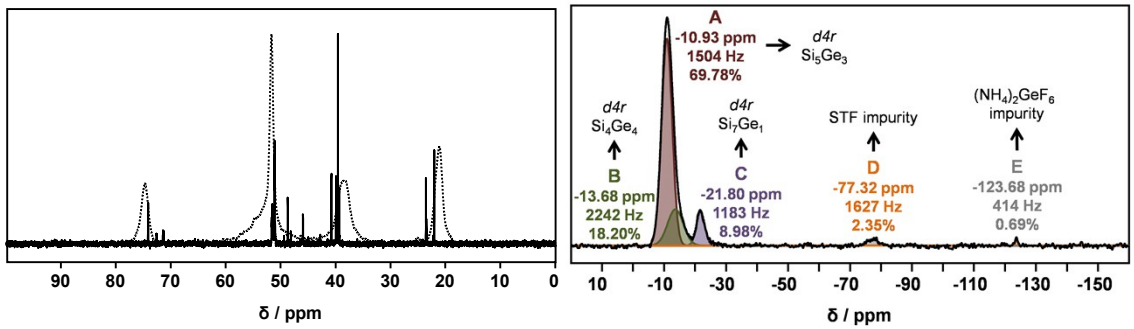

Figure S4: (CP) ^{13}C–NMR spectra (left) and ^{19}F–MAS–NMR spectrum of the zeolite ITQ-62 (right). In the ^{13}C MAS-NMR, the dotted lines correspond to the experimental spectrum from the obtained solid ^{1}H→^{13}C CP-MAS-NMR measurement, and the solid lines correspond to the liquid ^{13}C NMR spectrum of the OSDA dissolved in water. Also, the assignation of the ^{19}F resonances is shown. In the ^{19}F MAS-NMR spectra, solid lines correspond to the experimental spectrum, while dotted lines correspond to the sum of the deconvoluted spectra. Each deconvoluted signal is colored and named with a letter and their parameters (chemical shift in ppm, line width in Hz and integration).

Electron diffraction tomography analysis of the zeolite ITQ-62

Prior to the measurement, a small amount of the OSDA-containing sample was dispersed in dicloroethane and a drop of the suspension was deposited on a carbon-coated copper grid, that was mounted on a high tilt angle holder.

Electron diffraction patterns were collected using a microscope JEOL JEM-2100F with field emission gun operating at 200 kV. The patterns were obtained in parallel illumination, using the smallest C2 aperture ($10\ \mu m$).

The microscope is equipped with a Nanomegas Digistar P1000 device, which allows coupling electron diffraction tomography (EDT) with the precession of the electron beam. Using this experimental configuration reduces the dinamical effects on the EDT collected data and yields to intensities that are closer to their kinematical values. Diffraction patterns were obtained with a beam precession semi-angle of 0.7º.

The diffraction patterns were recorded with a GATAN Orius SC600A CCD camera at regular time intervals during sample rotation throughout an angular range of 50º around the tilt axis. The TEM image of the measured crystal is shown in Fig. S5.

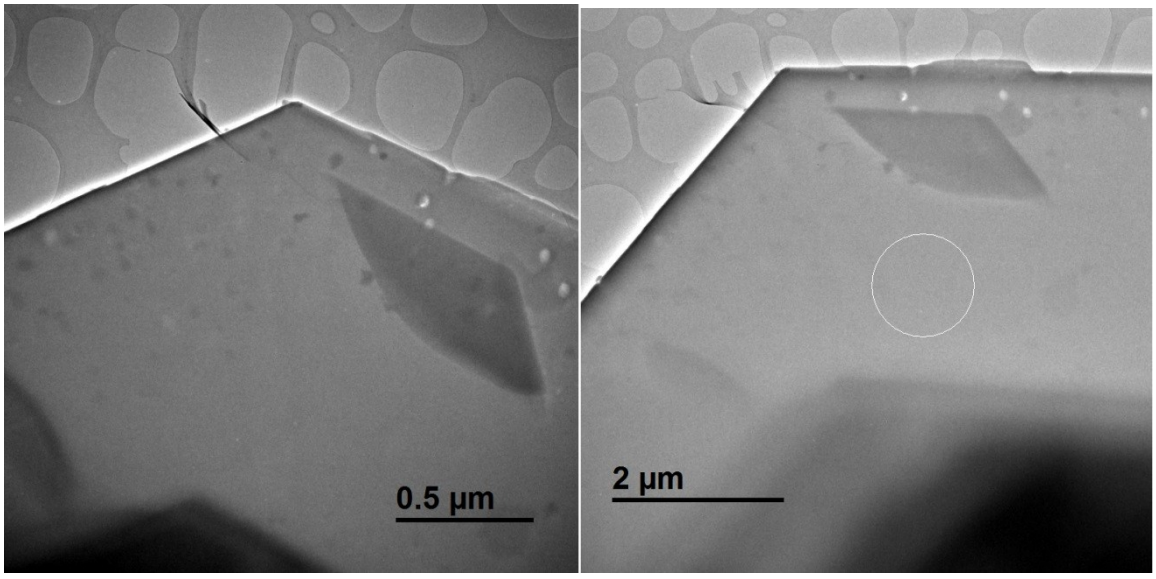

Figure S5: TEM image of the ITQ-62 crystal used for the structure determination. The white circle (left) indicates the measured region.

The series of collected patterns were processed with the program ADT3D. After the reconstruction of the three-dimensional reciprocal space and the determination of the unit cell, the integrated intensities of the measured reflections were extracted. The obtained unit cell parameters are given in Table S2. Projections of the reconstructed reciprocal space are shown in Fig. S6.

Table S2. Main crystallographic and collection data corresponding to the EDT analysis.

Compound	ITQ-62
Crystal data	
Crystal system	orthorhombic
Space group	*Cmmm*
Temperature (K)	295
a (Å)	20.61
b (Å)	17.92
c (Å)	7.62
α (º)	90.8
β (º)	89.6

γ (º)	89.3
V (Å^3)	2759.7
Collection data	
Wavelength (Å)	0.0251
Tilt angles	
Initial (º)	24.4
Final (º)	-39.8
Angular step (º)	0.9
No. all refl.	7182
No. unique refl.	928
Resolution (Å)	0.78
Coverage (%)	52
R_{sym} (on |F|) (%)	37.97

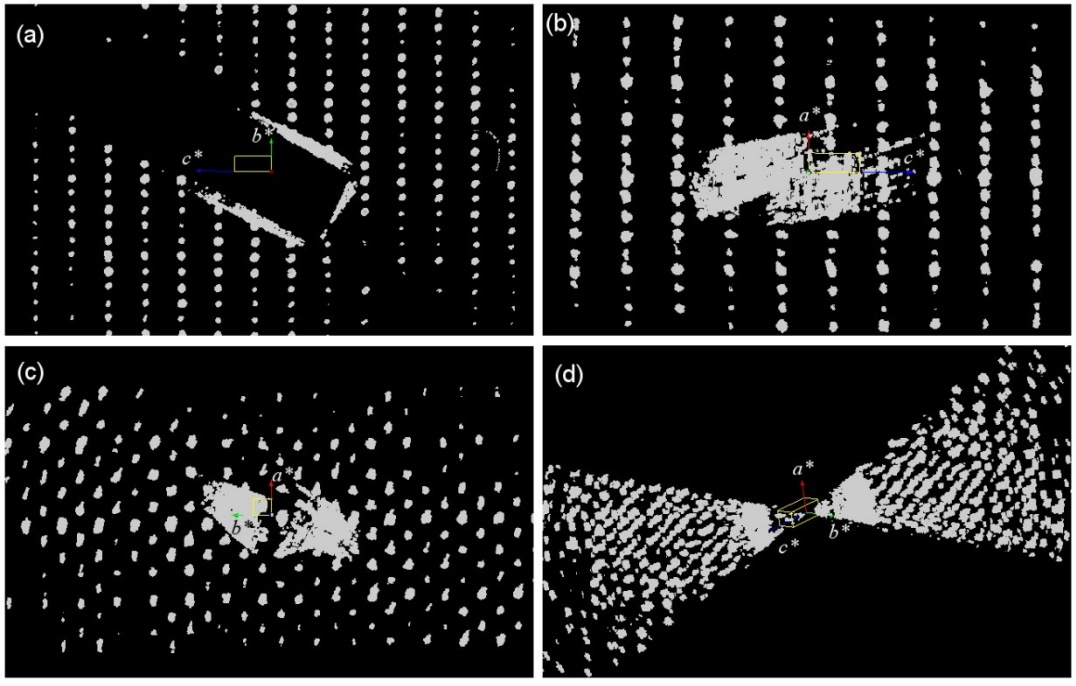

Figure S6: 3D projections of the reconstructed reciprocal space. (a) View along **a***, (b) along **b***, and (c) along **c*** directions. (d) View along the tilt axis.

Synchrotron XRPD analysis

XRPD data were collected at the beamline MSPD from the synchrotron ALBA using a Mythen detector and a wavelength of 0.61947(3) Å in an standard configuration. Total acquisition time was 45 min. Measurements were performed at room temperature, with the calcined sample sealed in a rotating capillary.

The intensities were extracted using the program FullProf, and the structure was solved using the program FOCUS. The results obtained proved to be identical to those obtained using EDT.

Attempts to solve the structure of ITQ-62 using the data corresponding to the as-made material did not give any reasonable result, contrasting with the Ultra-fast EDT technique were the presence of occluded OSDA filling the pores did not precluded the structure solution.

Laboratory XRPD data collection

Difractometer: PANalytical X'Pert PRO

Detector: PANalytical X'Celerator

Geometry: Bragg-Bretano geometry

X-ray radiation: Cu K_α (λ_1 = 1.5406 Å, λ_2 = 1.5444 Å, I_2/I_1 = 0.5)

Divergence slit: fixed = 1/16 º

Goniometer arm length: 240 mm

Tube voltage and intensity: 45 kV, 40 mA

Temperature: 303 K

Scan range: 3.0 º to 75.0 º (2θ); scan step size: 0.017 º (2θ); counting time: 3663 s/step.

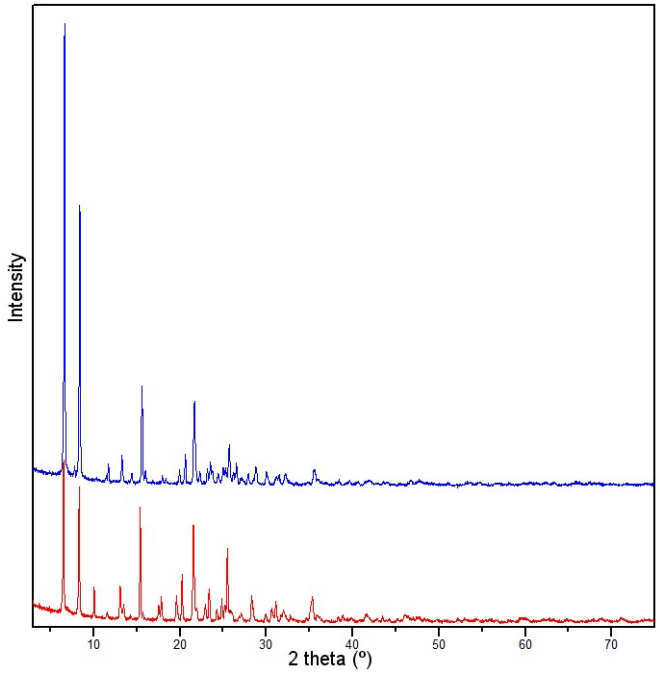

Figure S7: Laboratory XRPD patterns of as-made (bottom) and calcined (top) ITQ-62

Crystallographic refinement data for ITQ-62

Chemical formula: $Si_{0.75}Ge_{0.25}O_2$

Refined formula: $Si_{0.77}Ge_{0.23}O_2$

Space group: *Cmmm* (n. 65)

a = 21.1442(15) Å; *b* = 17.2655(13) Å; *c* = 7.5851(5) Å

V = 2769.1(3) $Å^3$; Z = 48

2θ range = 3-65 º; stepsize (2θ º) = 0.017 º

Regions excluded (2θº): 7.50º-7.90º, 11.30º-11.55º, 18.25º-18.50º, 26.35º-26.75º, 27.57º-28.14º

Peak range in FWHM = 25

Number of points = 3647; number of contributing reflections = 1331

Number of structural parameters = 35; number of profile parameters [(a)] = 12

Number of geometric restraints (d_{Si-O}=1.610(5) Å) = 15

Number of geometric restraints (d_{Ge-O}=1.740(5) Å) = 15

Number of geometric restraints (d_{T-T}=3.070(1) Å) = 10

Number of geometric restraints (d_{O-O}=2.629(25) Å) = 19

R_{wp} = 0.153; R_{exp} = 0.047; R_B = 0.069; R_F = 0.072

[(a)] Including zero-shift and unit cell parameters.

Table S3: Atomic coordinates, thermal parameters and occupancy for ITQ-62

Space group: *Cmmm*; *a* = 21.1442(15) Å; *b* = 17.2655(13) Å; *c* = 7.5851(5) Å

T-site	Atom	x[(a)]	y[(a)]	z[(a)]	U_{iso}[(b)]	Occupancy	Multiplicity & Wyckoff
T1	Si	0.12260(4)	0.08902(4)	0.20269(8)	0.0105(12)	0.656(6)	16r
	Ge					0.344(6)	
T2	Si	0.23193(4)	0.41097(4)	0.20270(8)	0.0105(12)	0.704(6)	16r
	Ge					0.296(6)	
Si3	Si	0.19012(3)	0.30036(5)	½	0.0105(12)	1	8q
T4	Si	0.07276(3)	0.19444(6)	½	0.0105(12)	0.871(8)	8q
	Ge					0.129(8)	
O1	O	0.1132(8)	0.1175(8)	0	0.039(4)	1	8p
O2	O	0.0985(6)	0	0.225(3)	0.039(4)	1	8o
O3	O	0.0765(4)	0.1425(5)	0.3226(7)	0.039(4)	1	16r
O4	O	0.19498(17)	0.0954(7)	0.2729(10)	0.039(4)	1	16r
O5	O	0.2080(7)	½	0.234(2)	0.039(4)	1	8o
O6	O	0.1897(4)	0.3521(4)	0.3245(7)	0.039(4)	1	16r
O7	O	0.2227(10)	0.3792(7)	0	0.039(4)	1	8p
O8	O	0.11878(14)	0.2696(2)	½	0.039(4)	1	8q
O9	O	¼	¼	0.5649(15)	0.09(3)	½[(c)]	8m
O10	O	0	0.2261(8)	½	0.039(4)	1	4j

Numbers in parentheses are the esd's in the units of the least significant digit given. [(a)] Parameters without an esd were not refined. Coordinates equal to 0, ¼ or ½ are fixed by symmetry. [(b)] All the T atoms have been refined with a common U_{iso} parameter; the same applies for all the O atoms, except O9. [(c)] U_{iso} of O9 was refined independently and its occupancy was set to ½ due to disorder.

Interatomic bond distances. All values in Å.

T1-O3=1.6217(77) | T1-O4=1.6242(44) | T1-O1=1.6263(47) | T1-O2=1.6281(47) — T1-O=1.6251

T2-O5=1.6356(51) | T2-O6=1.6383(70) | T2-O4=1.6383(43) | T2-O7=1.6440(48) — T2-O=1.6391

T3-O8=1.5992(31) | T3-O6=1.6032(59) | T3-O6=1.6032(59) | T3-O9=1.6129(35) — T3-O=1.6046

T4-O3=1.6190(65) | T4-O3=1.6190(65) | T4-O8=1.6220(34) | T4-O10=1.6327(47) — T4-O=1.6232

(Expected values taking into account the Si/Ge ratio: 1.65, 1.65, 1.61 and 1.63, respectively)

T-O-T and O-T-O angles. All values in °.

T1-O1-T1=141.934(30) | T1-O2-T1=141.486(35) | T4-O3-T1=144.182(424)
T1-O4-T2=141.055(242) | T2-O5-T2=140.037(34) | T3-O6-T2=144.188(401)
T2-O7-T2=138.519(30) | T3-O8-T4=146.260(215) | T3-O9-T3=144.458(25)(*)
T4-O10-T4=140.879(32)

O3-T1-O4=110.112(337) | O3-T1-O1=106.534(192) | O3-T1-O2=106.923(307)
O4-T1-O1=113.867(218) | O4-T1-O2=108.958(218) | O1-T1-O2=110.209(38)

O5-T2-O6=109.427(245) | O5-T2-O4=107.923(219) | O5-T2-O7=114.367(39)
O6-T2-O4=106.811(336) | O6-T2-O7=104.814(190) | O4-T2-O7=113.175(218)

O8-T3-O6=100.360(286) | O8-T3-O6=100.360(286) | O6-T3-O6=112.269(273) (*)

O3-T4-O3=112.432(273) | O3-T4-O8=114.447(286) | O3-T4-O10=103.384(293)
O3-T4-O8=114.447(286) | O3-T4-O10=103.384(293) | O8-T4-O10=107.304(111)

(*) T3-O9(averaged position)-T3=180.000º. O9-T3-O angles have been omitted due to the disorder of O9.

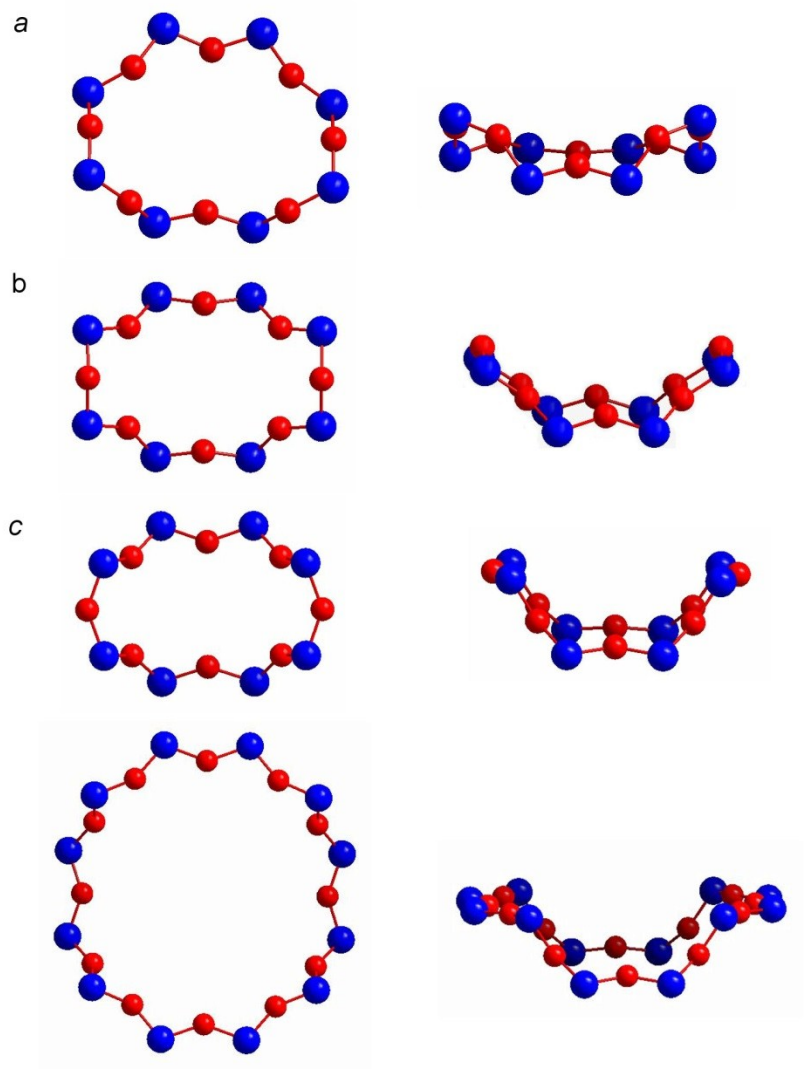

Figure S8: Channel openings in ITQ-62. (a) 8R channels along the *a* axis (3.9 Å x 2.4 Å), (b) 8R channels along the *b* axis (4.9 Å x 2.1Å), (c) 8R (top) and 12R (bottom) channels along the *c* axis (5.1 Å x 1.5 Å and 6.8 Å x 6.1 Å), respectively

References

45. C. A. Fyfe, D. H. Brouwer, A. R. Lewis, L. A. Villaescusa and R. E. Morris, *Journal of the American Chemical Society* 2002, **124** (26), 7770-7778.

46. A. Pulido, G. Sastre and A. Corma, *ChemPhysChem* 2006, **7** (5), 1092-1099.

47. J. A. Vidal-Moya, T. Blasco, F. Rey, A. Corma and M. Puche, *Chemistry of materials* 2003, **15** (21), 3961-3963.

48. X. Liu, Y. Chu, Q. Wang, W. Wang, C. Wang, J. Xu and F. Deng, *Solid State Nuclear Magnetic Resonance* 2017, **87**, 1-9.